Annals of Anatomy 224 (2019) 161–171

Contents lists available at ScienceDirect

Annals of Anatomy

journal homepage: www.elsevier.com/locate/aanat

Research article

# Anatomy, immunohistochemistry, and numerical distribution of human splenic microvessels

S. Almenar[a], C. Rios-Navarro[b], M. Ortega[a], P. Molina[a,c], A. Ferrandez-Izquierdo[a,b], A. Ruiz-Sauri[a,b,*]

[a] Department of Pathology, Faculty of Medicine, Universitat de Valencia, Valencia, Spain
[b] Institute of Health Research INCLIVA, Valencia, Spain
[c] Forensic Pathology Service, Institute of Legal Medicine and Forensic Sciences, Valencia, Spain

ARTICLE INFO

*Article history:*
Received 27 February 2019
Received in revised form 3 May 2019
Accepted 6 May 2019

*Keywords:*
Spleen
Vascularization
Immunohistochemistry
Morphometric analysis

ABSTRACT

The microvascular architecture of the spleen plays an important role in the immunological function of this organ. The different types of vessels are related to different reticular cells each with their own immunomodulatory functions.

The present study describes an immunohistochemical and morphometric analysis of the various types of vessels in 21 human autopsy non-pathological splenic samples.

On an area of 785,656.37 $\mu m^2$ for each sample, we classified and quantified the type and number of vascular structures, each according to their morphology and immunohistochemical profile, and obtained the ratios between them. The distribution of trabecular vessels and the characteristics of the venules are reviewed. In our material the so-called "cavernous perimarginal sinus" (anatomical structure previously described by Schmidt et al., 1988) was observed and interpreted as a curvilinear venule shaped by the follicle in contact with the trabecular vein.

Our material comprised 261 trabeculae (containing 269 arterial sections and 508 venous sections), 30,621 CD34+ capillaries, 7739 CD271+ sheathed capillaries, 2588 CD169+ sheathed capillaries, and 31,124 CD8+ sinusoids.

The total area (TA) (14,765,714.88 $\mu m^2$) occupied by the sinusoidal sections of the 21 cases was much higher than the TA of the capillary sections (1,700,269.83 $\mu m^2$). Similarly, the TA (651,985 $\mu m^2$) occupied by the sections of the trabecular veins was much higher than the TA of the trabecular arteries (88,594 $\mu m^2$).

The total number of CD34+ capillaries and of sinusoids CD8+ was similar for the sum of the 21 cases, nevertheless there were large differences in each case. Statistically the hypothesis that the number of capillaries and sinusoids are present with the same frequency is discarded.

In view of the absence of a numerical correlation between capillaries and sinusoids, we postulate that very possibly the arterial and the venous vascular trees are two anatomically independent structures separated by the splenic cords.

We believe that this is the first work where splenic microvascularization is simultaneously approached from a morphometric and immunohistochemical point of view.



## 1. Introduction

The spleen is an encapsulated and trabeculated organ formed by vessels and a special stroma that supports a large population of migratory blood cells (Tablin et al., 2002). In humans, the primary branches of the splenic artery and the polar arteries (both providing blood to the splenic segments) give rise to the subsegmental arter-

*Abbreviations:* α-SMA, alpha smooth muscle actin; Co, corona; FDCs, follicular dendritic cells; FRCs, fibroblastic reticular cells; Fs, lymphatic follicles; GC, germinal center; MZ, marginal zone; iMZ, inner marginal zone; oMZ, outer marginal zone; MRCs, marginal reticular cells; PALS, peri-arteriolar lymphatic sheath; iPALS, inner peri-arteriolar lymphatic sheath; oPALS, outer peri-arteriolar lymphatic sheath; PFZ, peri-follicular zone; RCs, reticular cells; SALs, sheath-associated lymphocytes; SAMs, sheath-associated macrophages; SCs, sheathed capillaries; TA, total area; WP, white pulp.

* Corresponding author at: Department of Pathology, University of Valencia, INCLIVA, Avda Blasco Ibáñez 15, Valencia, Spain.

*E-mail address:* Amparo.Ruiz-Sauri@uv.es (A. Ruiz-Sauri).

https://doi.org/10.1016/j.aanat.2019.05.004
0940-9602/

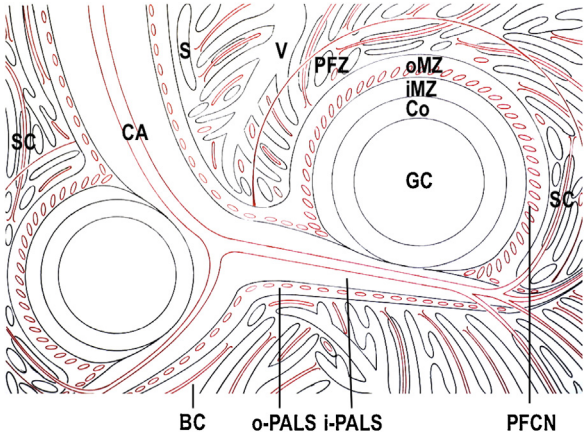


**Fig. 1.** Schematic representation of spleen histology. The two central arterioles run through the left and bottom ends of the image. Surrounding the periarteriolar connective tissue is the Inner Peri-Arteriolar Lymphatic Sheath (I-PALS). This thymus-dependent territory of white pulp is made up of fibroblastic reticular cells that support the T lymphocytes. When approaching the follicle, there is a progressive thinning that blurs this territory. The follicles correspond to B zone of the white pulp and contain Follicular Dendritic Cells that support both the mantle and the germinal center. The marginal zone constitutes the peripheral envelope of the white pulp and covers both the follicular mantle and the inner-PALS.
Abbreviations: BC: Billroth cord. CA: central arteriole. CO: corona. GC: germinal center. iMZ: inner marginal zone. iPALS: inner peri-arteriolar lymphatic sheath. oMZ: outer marginal zone. oPALS: outer peri-arteriolar lymphatic sheath. PFCN: peri-follicular capillary network. PFZ: peri-follicular zone. S: sinusoid. SC: sheathed capillary. V: venule.

ies, from which the sub-subsegmental arteries penetrate into the splenic parenchyma and constitute the trabecular arteries (Mikhail et al., 1979; Katritsis et al., 1982; García-Porrero and Lemes, 1988; Ignjatovic et al., 2005). From these structures the central arterioles originate (devoid of trabecular stroma) and form the axis of the splenic White Pulp (WP) (Fig.1). In humans the WP is composed of the Peri-Arteriolar Lymphatic Sheath (PALS), the lymphatic follicles and the Marginal Zone (MZ).

The PALS is located around the central arterioles. The inner portion of the PALS (iPALS) is equipped with a scaffold of Fibroblastic Reticular Cells (FRCs) CD271+ (Steiniger, 2015). These cells support a population of CD4 and CD8 T lymphocytes. In the vicinity of follicles, the T cells of the human iPALS are often asymmetrically distributed around the arterioles (Steiniger and Barth, 2000). The outer PALS (oPALS) contains α-SMA+ RCs that hold recirculating naïve B lymphocytes. The RCs of the oPALS are similar to the RCs of the outer marginal zone (oMZ) of the follicle (Steiniger, 2015; Steiniger et al., 2018a,b) and, in particular, the entire human WP is peripherally delimited by α-SMA+ RCs (Pinkus et al., 1986; Satoh et al., 1997).

The lymphatic follicles can be primary or secondary, these latter consisting of a Germinal Center (GC) and a mantle or corona (Co). The follicles are supported by a scaffold formed by CD271+ Follicular Dendritic cells (FDCs) (Labouyrie et al., 1997; Steiniger et al., 2014b). Outside these structures is found the Marginal Zone (MZ) of the follicle. In humans, the delimitation, composition and structure of the MZ has always been problematic. In addition, the size, composition, and even the presence or absence of the MZ may vary depending on certain pathological conditions (Schmidt et al., 1991). Nevertheless, a working model can be used considering that the inner Marginal Zone (iMZ) (in contact with the follicle) is supported by MAdCAM1+/SMA− Marginal Reticular Cells (MRCs) and the outer Marginal Zone (oMZ) by MAdCAM1+/SMA+ MRCs (the zone containing the perifollicular capillary network). Furthermore, the Reticular Cells (RCs) of the deeper portion of the oMZ express αSMA with greater intensity (MAdCAM1+/SMA++ MRCs) (Steiniger et al., 2018a,b).

Outside the MZ of the follicle there is the Peri-Follicular Zone (PFZ) (Van Krieken and te Velde, 1986, 1988; Steiniger et al., 2001) containing sheathed capillaries (SCs) and blood-filled spaces without endothelial lining.

When the central arterioles leave the WP, they become penicillar arterioles (arterioles of the red pulp) that give rise to the Sheathed Capillaries (SCs) and non-SCs that end in the splenic cords of the red pulp. The capillaries have either an open funnel-like end or a saccular expansion with discontinuities in its wall that permit blood cells and plasma to exit laterally into the surrounding reticular meshwork (Irino et al., 1977; McCuskey and Reilly, 1984 Fujita et al., 1992).

The endothelial cells of the SCs are covered externally by a layer of specialized cuboidal cells (Buyssens et al., 1984) that stain positively for anti-CD271 (Steiniger et al., 2014a). Outside these specialized stromal cells are the Sheath-Associated Macrophages (SAMs) and Sheath-Associated Lymphocytes (SALs). Most SAMs are CD68+CD163−CD169− and only those macrophages in the perifollicular SCs are CD169+ (Steiniger et al., 1997, 2014a). The SALs are B lymphocytes IgM+IgD++ and switched cells (Steiniger et al., 2014a). According to Steiniger et al. (2018b) the sheathed capillaries of the human spleen could attract B lymphocytes from the red pulp to the arteriolar branches to reach the follicles. It seems that the SCs and non-SCs (both located inside the Billroth cords) do not have anatomical continuity with the venous sinusoids (Steiniger et al., 2011). The endothelial cells of sinusoids have a barrel stave morphology and a peculiar immunohistochemical expression of the alpha monomer of the CD8 co-receptor, as demonstrated by Stuart and Warford (1983) with anti-OKT8. "There may be venules forming a connection between sinuses and trabecular veins, but these vessels are extremely short" (Steiniger and Barth, 2000). Finally, with regard to venous return, Dawson et al., 1986 shows that the venous vascular structure of the spleen is also of a segmentary nature and pointed out that "when arteries and veins were both injected, similar segmentation was noted".

However, the numerical distribution of the different types of splenic vessels and the topographical relationship with respect to certain splenic structures is not well known. In this regard, the venules of the red pulp have received scant attention with respect to their morphology, size, anatomical relations with the trabecular veins, and the antigenic profile of their endothelium.

For these reasons we performed a quantitative study of these structures based on their immunohistochemical markers.

## 2. Material and methods

### 2.1. Study population and spleen tissue samples

Formalin-fixed, paraffin-embedded spleen tissues were retrieved from 25 forensic autopsies between 2008 and 2011. All the procedures carried out with the splenic samples of these autopsies were in accordance with the Declaration of Helsinki. At the time of death, these patients had no clinical or analytical alterations suggestive of haematological or infectious disease.

For each of these 25 paraffin blocks, 10 anonymized 6μm-thick sections were taken. Furthermore, histological confirmation (with conventional H&E stain) in order to exclude any splenic parenchymal structural alteration was performed. Four cases were ruled out due to alterations either in morphology or in the antigenicity of CD8 in the splenic sinusoids. Thus, the anonymized preparations of 21 cases were used for the study.

**Table 1**
This table shows the different antibodies, the name of the clone, manufacturer and additional specifications.

| | Factory | Clone | Antigen retrieval | Concentration |
|---|---|---|---|---|
| Anti-CD34 | Abcam | EP373Y | High | 1:100 |
| Anti-CD31 | Dako | JC70A | Pretreatment with PTlink | prediluted |
| Anti-CD271 | LSBio | | Low | 1:100 |
| Anti-CD169 | Abcam | SP216 | High | 1:100 |
| Anti-MAdCAM-1 | Abcam | 314G8 | Low | 1:50 |
| Anti-SMA | Dako | 1A4 | Pretreatment with PTlink | prediluted |
| Anti-CD8 | Dako | C8/144B | Pretreatment with PTlink | prediluted |

### 2.2. Histological criteria

The histological criteria of Van Krieken and te Velde (1988), Steiniger and Barth (2000), and Tablin et al. (2002) were used to identify the different structures of the human spleen.

### 2.3. Sample staining

The immunohistochemical protocol was carried out by the standardized DAKO Autostainer system for anti-CD8, anti-CD31, and anti-SMA. For anti-CD169, anti-MAdCAM-1, and anti-CD271, antigen retrieval was performed by autoclave incubation for 3 min at 1.5 atmospheres with citrate buffer pH 6.1. The sections were washed three times in Tris Buffered Saline. The peroxidase activity was visualized using 3,3-diaminobenzidine and imidazole (0.01) as chromogen (see Table 1). Anti-CD34, anti-CD31, anti-CD271, anti-CD169, and anti-CD8 antibodies are used to obtain qualitative and quantitative results. On the other hand, anti-MAdCAM-1 and anti-SMA are used to obtain only qualitative results.

### 2.4. Image analysis

All the slides were examined at low magnification (5×) to select fields with better preserved morphology. For each of these twenty-one cases, ten photographic images were taken with a Leica DMD3000 microscope (Leica Microsystems, Wetzlar, Germany) at 10× magnification. An area of 707,313.53 $\mu m^2$ was scanned each for microphotograph. Thus, a TA of 7,073,135.3 $\mu m^2$ was covered in each case. All the photographic images were analyzed using Image-Pro Plus 7.0 software (Media Cybernetics, Silver Spring, MD, USA).

To measure the number of capillaries marked with anti-CD34 and also the TA that they occupy, the image was transformed to gray scale. Subsequently, the image was segmented with limits from 0 to 110 on the color palette. In this way, all the capillaries are marked in red. To eliminate background noise the system was programmed to remove spaces with a minimum diameter under 5 μm. In the same way, to measure the number and TA of trabecular veins and arteries marked with anti-CD31, the image was segmented with limits from 0 to 101, but delimiting manually the area to be measured.

To quantify the number of capillaries marked with anti-CD271 and anti-CD169, the images were respectively segmented with limits from 0 to 145 and from 0 to 122.

To measure the number of sinusoids marked with anti-CD8 and also the area that they occupy, the image was segmented with limits from 0 to 116. Taking into account that some sinusoidal vessels are not closed, they become closed curves with the "Draw Objects" function. There is a small measurement error because some lymphocytes or dendritic cells (which are marked with anti-CD8) are attached to vascular structures and the morphometric program considers them as excrescences or irregularities of the blood vessel.

### 2.5. Statistical analysis

We made an appropriate frequency estimation using the Chi-Square Test Statistic

$$\chi^2 = \sum_{i=1}^{n} \frac{(O_i - E_i)^2}{E_i}$$

where $O_i$ was the observed value of a given variable in the i-th case, $E_i$ is the expected value (given that $H_0$ is true) of that same variable in the i-th case and $n$ the total number of studied cases (Daniel and Cross, 2013).

## 3. Results

### 3.1. CD34

Qualitative results: anti-CD34 stained the endothelial cells of the trabecular arteries and veins, cord arterioles, perifollicular and cord capillaries, perifollicular sinusoids (faintly), and cord venules as well as the fibroblasts of the adventitia of large vessels, subcapsular connective tissue, and trabeculae (Figs. 2, 3 A, 3 B). In our material (Fig. 2A), the innermost circumferential layer of capillaries, located within the marginal zone (made up of larger lymphocytes with lighter cytoplasm), stained with anti-CD34. These capillaries were closer to the follicular corona (mantle) than the CD271 capillaries and, as can be seen in the figure, they were located farther from the perifollicular sinusoids (which appeared very palely stained in the preparations).

The venules presented a different immunohistochemical profile to the sinusoids, although, from a morphological point of view, the venules seemed to be a gradual continuation of these. Unlike sinusoids, they presented a clear CD34 expression (Fig. 2B).

Quantitative results: in 210 (10 × 21) photomicrographs (148,535,841.3 $\mu m^2$) there were 30,621 CD34+ capillaries (206.15/$mm^2$). In 7,073,135.3 $\mu m^2$ (area of each case) there was a mean of 1458.14 CD34+ capillaries [15 cases in the interval (1193.31–1722.97) ($\mu + 1\sigma$)] and the mean of the area occupied by the CD34 capillaries was 80,965.23 $\mu m^2$ [19 cases in the interval (57,737.97–104,192.49) ($\mu + 1\sigma$)] (Tables 2 and 3).

### 3.2. CD31

Qualitative results: in our material anti-CD31 (PECAM-1 Platelet/Endothelial Cell Adhesion Molecule-1) stained the vascular endothelium of all splenic vascular structures (including the endothelium of the splenic sinusoids) (Fig. 3C). This immunostaining revealed the vascular swarm of the marginal and perifollicular zones. (Fig. 3D). In these areas there was a complicated warp of cells that partially obscured the view of the lumen. The endothelial cells of the sinusoids and cord venules were clearly marked. Furthermore, the red pulp capillaries stained with greater intensity than the sinusoids. Within the trabeculae the arteries stood out over the veins due to the greater height of their endothelium, although the arterial diameter was always less than that of the vein.

Quantitative results: in the total surface analyzed of the 21 cases we found 257 trabeculae containing 275 trabecular arterial sections and 540 trabecular venous sections. The venous sections occupied an area of 651,985 $\mu m^2$. The arterial sections occupied an area of 88,594 $\mu m^2$. The distribution of the different types of vascular sections within the trabeculae is shown in Table 4.

Fig.4 shows how the microphotograph stained with anti-CD31 was transformed for analysis with Image ProPlus.

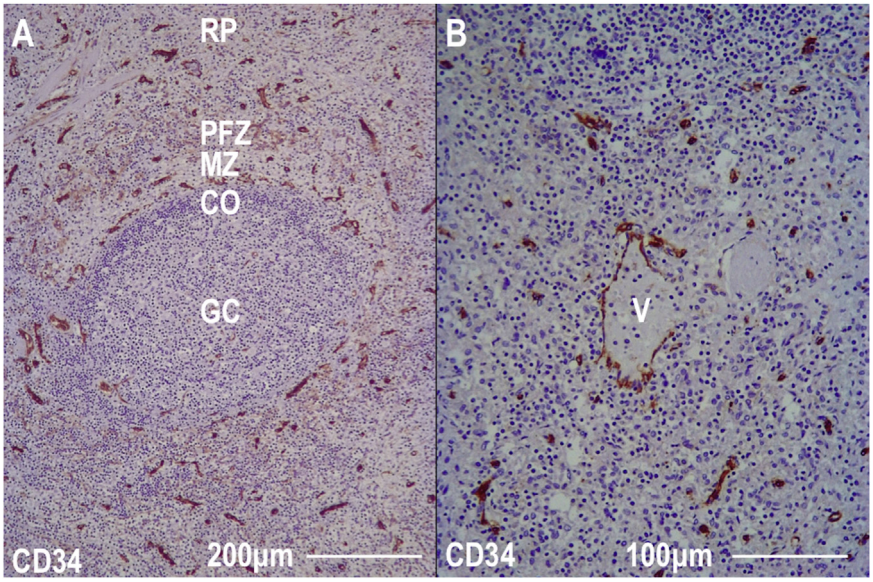


**Fig. 2.** (A) CD34. 10×. In the marginal zone, there are numerous vessels that constitute the "perifollicular capillary network". More externally, in the perifollicular territory, capillaries similar to those of the red pulp are appreciated. In this zone the perifollicular sinusoids also appear weakly stained. (B) CD34. 20×. In the central portion, a venule whose endothelium CD34+ lacks a connective sheath, is surrounded by a red pulp in which the sinusoids are not stained. Conversely, the capillaries show intense positivity with anti-CD34.
Abbreviations: CO: Corona. GC: Germinal Center. MZ: Marginal Zone. PFZ: Peri-Follicular Zone. RP: Red Pulp. V: Venule.

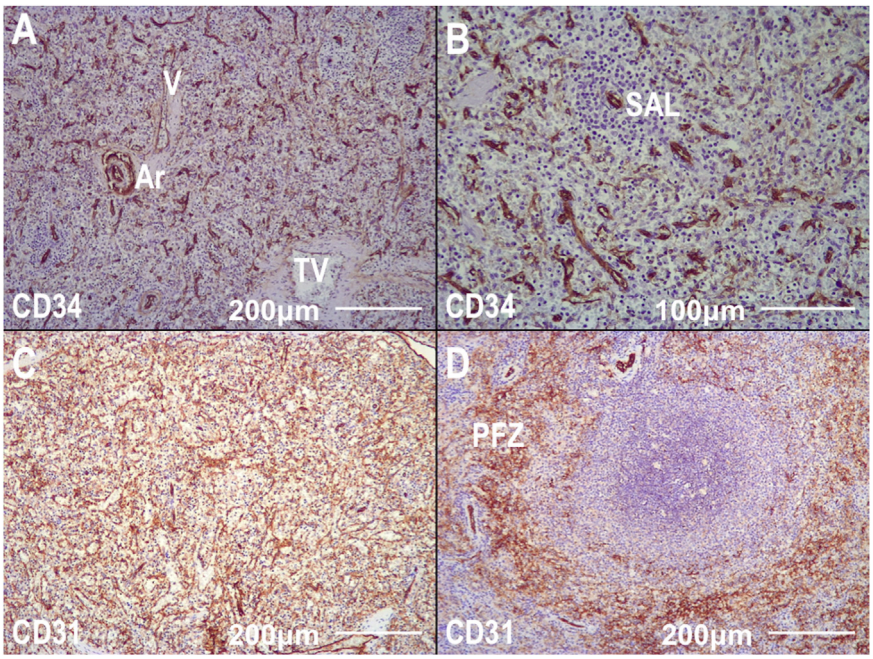


**Fig. 3.** (A) CD34. 10×. Immunostaining with anti-CD34 makes it possible to visualize the diffuse distribution of the capillaries throughout the red pulp. They appear as sharp individual thin ribbons of variable length (which facilitates counting with the function "manual tag" of "Image ProPlus"). There is a trabecular vein (TV), a cord venule (V) and an artery (Ar) whose periadventitial stroma is also marked with anti-CD34. (B) CD34. 20×. Several well individualized capillaries with defined lumens. This antibody highlights a capillary surrounded by a dense accumulation of lymphocytes that must be interpreted as Sheath-Associated Lymphocytes (SAL). (C) CD31. 10×. Anti-CD31 stains both capillaries and sinusoids. As can be seen (by comparison with the upper image) the microvascular density is very high, making it extremely difficult to identify each type of vessel. (D) CD31. 10×. Anti-CD31 stains an authentic swarm of microvessels throughout the wide band of the perifollicular zone (PFZ).

### 3.3. CD271

Qualitative results: in our material, with the 75 kDa low-affinity NGF receptor, an intense immunoreaction was observed in follicular dendritic cells and, in some cases, there was a clear fringe (marginal zone) that separated these cells from the perifollicular SCs. In addition, the SCs were observed throughout the red pulp. These capillaries were covered by cuboidal cells ("isoprimatics") that presented a sharp immunoreaction with this marker (Fig. 5A).

Quantitative results: at 148,535,841.3 $\mu m^2$ there were 7739 CD271 positive SCs (52.1/$mm^2$). At 7,073,135.3 $\mu m^2$ (area of each case) there was a mean of 368.52 CD271 positive SCs [13 cases in the interval (278.46–458.57) ($\mu + 1\sigma$)] (Table 2).

**Table 2**
The quantities for each of the boxes correspond to the measurement of one case (7,073,135.3 $\mu m^2$). The number of capillaries CD34+, CD8+ sinusoids, ratio between both quantities, sheathed capillaries CD271+, proportion of capillaries CD271+ with respect to the total number of capillaries, sheathed capillaries CD169+, proportion of capillaries CD169+ with respect to the total number of capillaries and proportion of both types of sheathed capillaries are expressed in the columns.

| | CD34 | CD8 | CD34/CD8 | CD271 | CD34/CD271 | CD169 | CD34/CD169 | CD271/CD169 |
|---|---|---|---|---|---|---|---|---|
| 1 | 1826 | 1932 | 0.945 | 457 | 3.995 | 127 | 14.377 | 3.598 |
| 2 | 1645 | 1537 | 1.070 | 433 | 3.799 | 152 | 10.822 | 2.848 |
| 3 | 1602 | 1763 | 0.908 | 202 | 7.930 | 114 | 14.052 | 1.771 |
| 4 | 1417 | 1524 | 0.929 | 497 | 2.851 | 96 | 14.760 | 5.177 |
| 5 | 1325 | 1245 | 1.064 | 284 | 4.665 | 119 | 11.134 | 2.386 |
| 6 | 966 | 1297 | 0.744 | 318 | 3.037 | 103 | 9.378 | 3.087 |
| 7 | 1535 | 1382 | 1.110 | 469 | 3.272 | 146 | 10.513 | 3.212 |
| 8 | 1398 | 1495 | 0.935 | 385 | 3.631 | 155 | 9.019 | 2.483 |
| 9 | 1901 | 1668 | 1.139 | 420 | 4.526 | 137 | 13.875 | 3.065 |
| 10 | 1294 | 1456 | 0.888 | 239 | 5.414 | 104 | 12.442 | 2.298 |
| 11 | 1341 | 1273 | 1.053 | 342 | 3.921 | 92 | 14.576 | 3.717 |
| 12 | 1229 | 1561 | 0.787 | 275 | 4.469 | 123 | 9.991 | 2.235 |
| 13 | 1408 | 1324 | 1.063 | 246 | 5.723 | 88 | 16.000 | 2.795 |
| 14 | 1346 | 1238 | 1.087 | 452 | 2.977 | 135 | 9.970 | 3.348 |
| 15 | 1387 | 1243 | 1.115 | 325 | 4.267 | 118 | 11.754 | 2.754 |
| 16 | 1325 | 1689 | 0.784 | 512 | 2.587 | 147 | 9.013 | 3.482 |
| 17 | 2072 | 1813 | 1.142 | 473 | 4.380 | 168 | 12.333 | 2.815 |
| 18 | 1125 | 1362 | 0.825 | 371 | 3.032 | 145 | 7.758 | 2.558 |
| 19 | 1776 | 1535 | 1.157 | 336 | 5.285 | 102 | 17.411 | 3.294 |
| 20 | 1321 | 1464 | 0.902 | 348 | 3.795 | 136 | 9.713 | 2.558 |
| 21 | 1382 | 1323 | 1.044 | 355 | 3.611 | 81 | 17.061 | 4.382 |
| S | 30,621 | 31,124 | | 7739 | | 2588 | | |
| $\mu$ | 1458.14 | 1482.09 | 0.98528 | 368.52 | 4.150 | 123.23 | 12.18 | 3.041 |
| $\sigma$ | 264.82 | 201.10 | 0.13062 | 90.05 | 1.222 | 24.50 | 2.81 | 0.766 |

**Table 3**
The quantities that appear in each box correspond to the surface (expressed in $\mu m^2$) occupied by the sinusoids and capillaries of a given case (7,073,135.3 $\mu m^2$). In the last column the proportion between both surfaces is expressed.

| | CD8 | CD34 | CD8/CD34 |
|---|---|---|---|
| 1 | 491,851 | 61,686 | 7.973 |
| 2 | 592,702 | 63,068 | 9.397 |
| 3 | 685,931 | 79,841 | 8.591 |
| 4 | 794,972 | 97,669 | 8.139 |
| 5 | 628,065 | 76,668 | 8.192 |
| 6 | 567,903 | 53,140 | 10.686 |
| 7 | 793,178 | 92,789 | 8.548 |
| 8 | 590,487 | 69,203 | 8.532 |
| 9 | 868,525 | 94,684 | 9.172 |
| 10 | 636,656 | 68,945 | 9.234 |
| 11 | 725,643 | 70,625 | 10.274 |
| 12 | 641,625 | 80,942 | 7.926 |
| 13 | 660,774 | 59,301 | 11.142 |
| 14 | 689,813 | 90,083 | 7.657 |
| 15 | 631,570 | 70,763 | 8.925 |
| 16 | 655,897 | 72,040 | 9.104 |
| 17 | 1,029,512 | 146,228 | 7.040 |
| 18 | 537,649 | 63,381 | 8.482 |
| 19 | 938,825 | 135,113 | 6.948 |
| 20 | 874,514 | 72,574 | 12.049 |
| 21 | 729,623 | 81,527 | 8.949 |
| Total | 14,765,715 | 1,700,270 | |
| $\mu$ | 703,129.28 | 80,965.23 | 8.902 |
| $\sigma$ | 136,968.04 | 23,227.26 | 1.278 |

### 3.4. CD169

Qualitative results: sialoadhesin (Siglec-1) is a macrophage restricted cell surface receptor (Van den Berg et al., 1992; O'Neill et al., 2012) which, in our study, was expressed on perifollicular SCs (Fig. 5B). At low magnification, it was found that fewer capillaries with an envelope react with anti-CD169 than anti-CD271. In many cases a clear band (presumably corresponding to the marginal zone) was observed between follicular cells and immunostained capillaries. When the network of CD169 SCs was denser, it was more difficult to observe the phenomenon described above.

Quantitative results: at 148,535,841.3 $\mu m^2$ there were 2588 CD169 positive SCs (17.42/$mm^2$). At 7,073,135.3 $\mu m^2$ (area of each case) there was a mean of 123.23 CD169 positive SCs [14 cases in the interval (98.73–147.73) ($\mu + 1\sigma$)] (Table 2).

### 3.5. MAdCAM-1

Mucosal vascular addressin expression was found on the scaffold of the marginal zone formed by the MRCs (Fig. 5C). The cells that reacted with this antibody had a fibroblastoid-reticular morphology and did not appear to be the features of endothelial cells.

### 3.6. SMA

The entire periphery of the WP was delimited by reticular-fibroblastoid cells that reacted intensely with anti-SMA (Fig. 5D).

**Table 4**
Numerical distribution of arteries and veins within the trabeculae. **0V/1A =** trabecula with an arterial section that does not contain any venous section . . . **4V/4A =** trabecula containing 4 venous sections and 4 arterial sections.

| | | | | | | |
|---|---|---|---|---|---|---|
| **0V/1A** | 5 | **2V/0A** | 16 | **3V/2A** | 25 | |
| **1V/0A** | 53 | **2V/1A** | 25 | **4V/1A** | 13 | |
| **1V/1A** | 29 | **2V/2A** | 10 | **4V/2A** | 16 | |
| **1V/2A** | 17 | **2V/3A** | 3 | **4V/3A** | 9 | |
| **1V/3A** | 3 | **3V/1A** | 29 | **4V/4A** | 4 | |
| | Trabeculae **107** | | Trabeculae **83** | | Trabeculae **67** | **257** |
| | Veins **102** | | Veins **195** | | Veins **243** | **540** |
| | Arteries **54** | | Arteries **83** | | Arteries **138** | **275** |

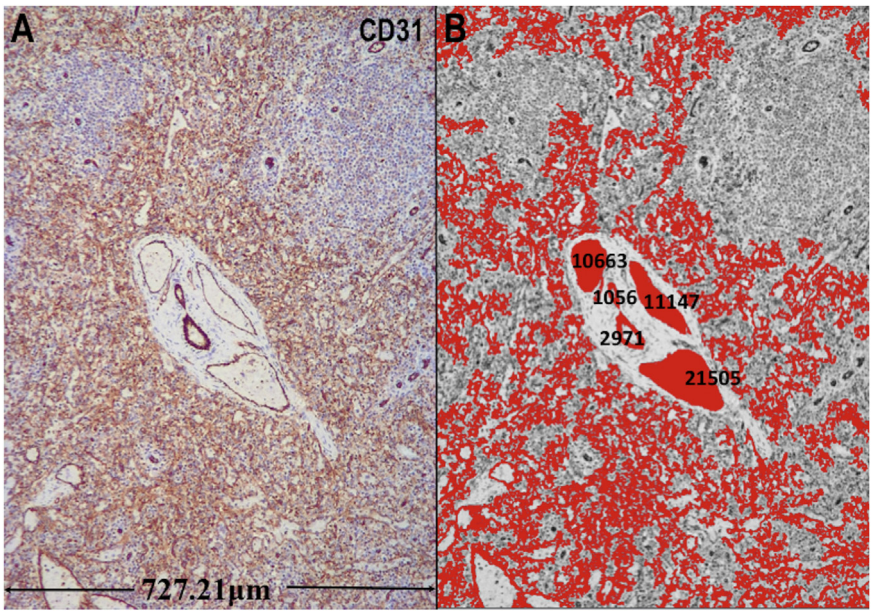


**Fig. 4.** (A) CD31. 10×. Immunostaining with anti-CD31 makes it possible to clearly identify the entire splenic vessels (including all trabecular vessels). (B) After applying the procedure described in Section 2 to the previous image with Image ProPlus, the area occupied by the sections of all trabecular vessels is obtained.

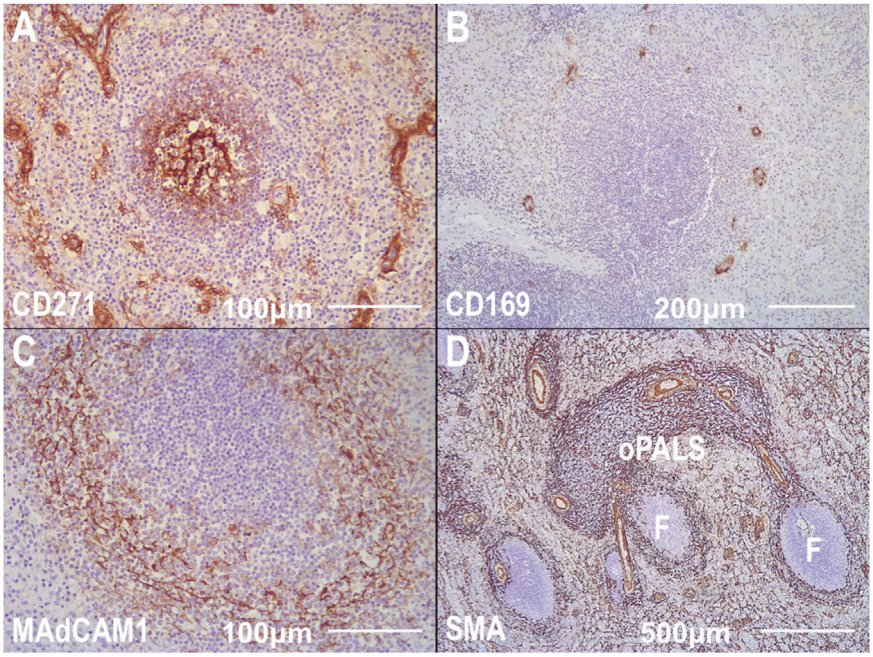


**Fig. 5.** (A) CD271. 20×. The follicular dendritic cells of the germinal center are more intensely stained with anti-CD271 than those found at the mantle (corona). Externally, a clear band corresponds to the MZ. More peripherally (in the perimarginal zone) appear the sheathed capillaries. The latter are not only found in perifollicular territory, since they can be seen anywhere in the red pulp. (B) CD169. 10×. Anti-169 reacts with the stromal cells of the sheathed capillaries predominantly located in the perifollicular area. (C) MAdCAM-1. 20×. All marginal zone (MZ) cells (both outer-MZ and inner-MZ cells) are stained with anti-MAdCAM-1. Observe how these cells appear intertwined and present a reticular-fibroblastoid morphology without delimiting sinusoidal vascular structures. (D) SMA 5×. The SMA+MRCs of myofibroblastic morphology provide a concentric network in the PALS. If the PALS is broad, the staining intensity for SMA is much higher in the outer-PALS (oPALS) than in the inner-PALS. The strongly SMA-positive myofibroblast network of the outer-PALS continues into the innermost SMA++ marginal reticular cells of the outer-MZ of the follicles as a rather thin structure (Steiniger et al., 2001, 2018a,b).

The most central portion of PALS (inner PALS) presented a lower intensity stain. This marker has been used primarily for the purpose of specifying the position of some white pulp structures.

### 3.7. CD8

Qualitative results: immunostaining with anti-CD8 clearly marked the endothelial cells of the splenic sinusoids (Fig. 6A, B) and numerous T lymphocytes located in the PALS, in the follicles and in the splenic cords. In various sections, the perifollicular sinusoids were separated from the follicle by a strip corresponding to the marginal zone. This marker did not react with the venules (which were labeled with anti-CD31 and anti-CD34).

Quantitative results: at 148,535,841.3 $\mu m^2$ there were 31,124 CD8 positive sinusoids (209.53/$mm^2$). At 7,073,135.3 $\mu m^2$ (area of each case) there was a mean of 1482.09 CD8 positive sinu-

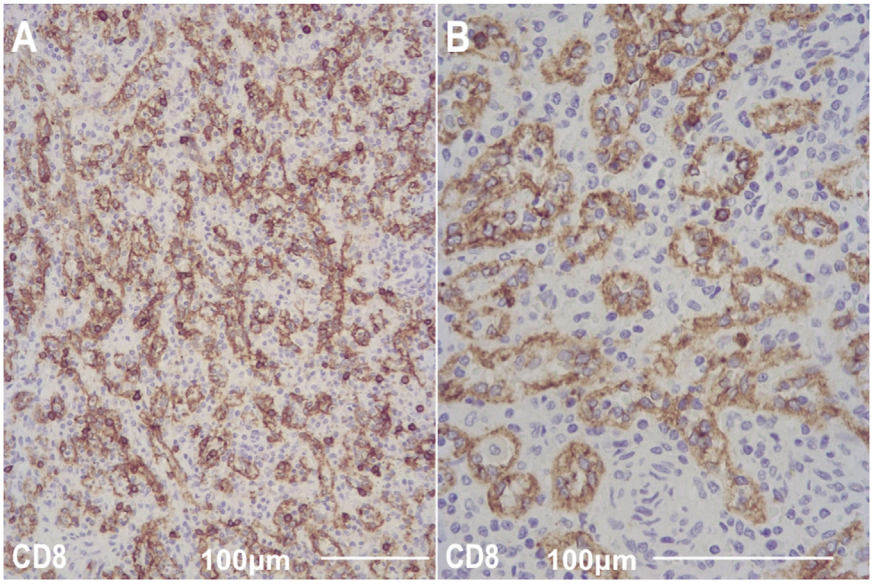


**Fig. 6.** (A) CD8. 20. Immunostaining with anti-CD8 makes it possible to identify all splenic sinusoids. These appear as vessels of broad lumen, more or less tortuous trajectory and variable length. However, this immunostaining also makes it possible to count such vessels with the "Manual Tag" function of "Image ProPlus". Within the splenic cords, CD8+ cells are observed, which may correspond to cytotoxic/suppressor T cells or dendritic cells. (B) CD8. 40×. In the cross sections of the endothelium of the sinusal cells have a cuboidal morphology determining a rosette-like arrangement of their nuclei.

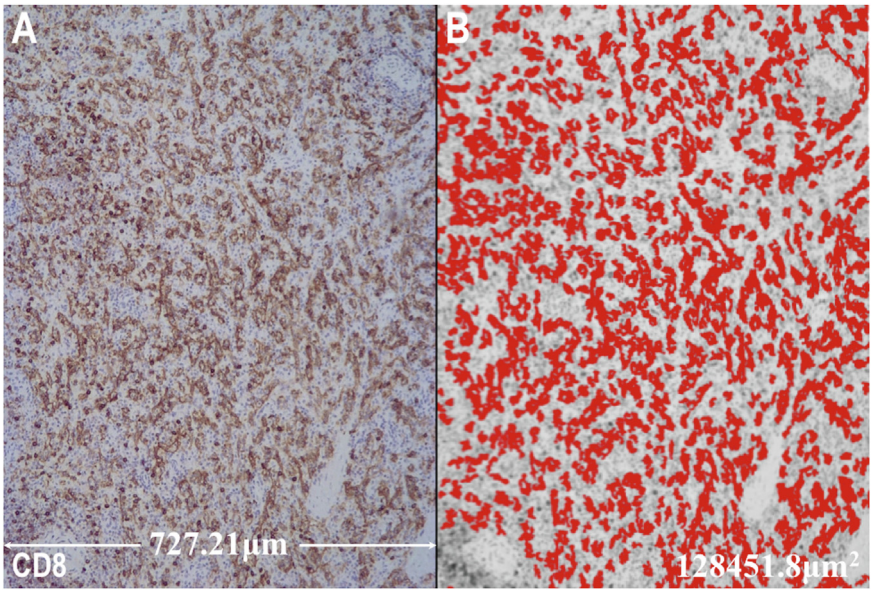


**Fig. 7.** (A) CD8. 10×. Immunostaining with anti-CD8 makes it possible to clearly identify the splenic sinusoids. (B) After applying the procedure described in Section 2 to the previous image with Image ProPlus, the area occupied by all the sinusoidal sections of this photomicrograph is obtained.

soids [13 cases in the interval (1280.99–1683.19) $(\mu + 1\sigma)$] and the mean of the area occupied by the CD8 sinusoids was 703,129.28 μm$^2$ [15 cases in the interval (566,161.24–840,097.32) $(\mu + 1\sigma)$] (Tables 2 and 3). Fig. 7 shows the microphotograph transformation for analysis with Image ProPlus.

### 3.8. Ratios of capillaries CD34, CD271 and CD169 (see Table 2)

The Within the interval

$$mean\ of\ \frac{capillaries\ CD34\ of\ the\ i-th\ case}{capillaries\ CD271\ of\ the\ i-th\ case} = 4.15080$$

Within the interval (2.9288–5.3728) $(\mu + 1\sigma)$ there are 16 cases.

$$mean\ of\ \frac{capillaries\ CD271\ of\ the\ i-th\ case}{capillaries\ CD169\ of\ the\ i-th\ case} = 3.04109$$

Within the interval (2.2750–3.8070) $(\mu + 1\sigma)$ there are 17 cases.

$$mean\ of\ \frac{capillaries\ CD34\ of\ the\ i-th\ case}{\sin usoids\ CD8\ of\ the\ i-th\ case} = 0.985285$$

**Table 5**
This table shows the 21 addends of the Chi-Square Test.

| | $C_i$ | $S_i$ | $E_i$ | $(C_i - E_i)^2/E_i = (S_i - E_i)^2/E_i$ |
|---|---|---|---|---|
| 1 | 1826 | 1932 | 1879 | 1.494944 |
| 2 | 1645 | 1537 | 1591 | 1.832809 |
| 3 | 1602 | 1763 | 1682.5 | 3.851560 |
| 4 | 1417 | 1524 | 1470.5 | 1.946446 |
| 5 | 1325 | 1245 | 1285 | 1.245136 |
| 6 | 966 | 1297 | 1131.5 | 24.207026 |
| 7 | 1535 | 1382 | 1458.5 | 4.012512 |
| 8 | 1398 | 1495 | 1446.5 | 1.626166 |
| 9 | 1901 | 1668 | 1784.5 | 7.605631 |
| 10 | 1294 | 1456 | 1375 | 4.771636 |
| 11 | 1341 | 1273 | 1307 | 0.884468 |
| 12 | 1229 | 1561 | 1395 | 19.753405 |
| 13 | 1408 | 1324 | 1366 | 1.291361 |
| 14 | 1346 | 1238 | 1292 | 2.256965 |
| 15 | 1387 | 1243 | 1315 | 3.942205 |
| 16 | 1325 | 1689 | 1507 | 21.980092 |
| 17 | 2072 | 1813 | 1942.5 | 8.633333 |
| 18 | 1125 | 1362 | 1243.5 | 11.292521 |
| 19 | 1776 | 1535 | 1655.5 | 8.770915 |
| 20 | 1321 | 1464 | 1392.5 | 3.671127 |
| 21 | 1382 | 1323 | 1352.5 | 0.643438 |
| | | | | 135.713696 |

Within the interval (0.8551–1.1159) ($\mu + 1\sigma$) there are 14 cases.

$$mean\ of\ \frac{surface\ occupied\ by\ \sin usiods\ CD8\ of\ the\ i-th\ case}{surface\ occupied\ by\ capillaries\ CD34\ of\ the\ i-th\ case} = 8.902$$

Within the interval (7.623–10.181) ($\mu + 1\sigma$) there are 15 cases.

### 3.9. Distribution of trabecular arteries and veins

See CD31 quantitative results.

### 3.10. Comparative distribution of capillaries CD34 and sinusoids CD8

Since the mean of CD34 capillaries was very similar to the mean of CD8 sinusoids, it would seem logical to ascertain if there is a statistical correlation between the frequencies observed in each of the 21 cases. Let us consider as $H_0$ hypothesis that, in each case, the number of capillaries CD34 and sinusoids CD8 are present with the same frequency and as $H_1$ hypothesis that it is different. If according to the $H_0$ hypothesis the number of capillaries ≈ number of sinusoids, then the expected value would be $E_i = (C_i + S_i)/2 \approx C_i \approx S_i$. ($C_i$ = *number of observed capillaries*; $S_i$ = *number of observed sinusoids*). With the aid of Table 5 we obtain $\chi^2 = 135.713696$. The system has $(2-1)\times(21-1) = 20$ degrees of freedom. If $\alpha = 0.005$ (the lowest tabulated value), then the critical value for 20 degrees of freedom is 39.9968. Since 39.9968 < 135.713696, the $H_0$ hypothesis is rejected.

## 4. Discussion

Three aspects of the human splenic structure have attracted the attention of numerous authors: The segmental nature of the splenic vessels (with predominantly surgical purposes) (Christo and DiDio, 1997), the continuity of arterial capillaries and venous sinusoids (reviewed by Fujita et al., 1992) and the nature of the MZ (reviewed by Steiniger and Barth, 2000; Steiniger et al., 2001, 2006; Weill et al., 2009).

According to a common representation in the histology texts, in each splenic trabecula there is a trabecular artery and a trabecular vein and this scheme is repeated from the juxta-hilar trabeculae up to the convex portion of the organ. In the sections closest to the splenic hilum, the most important arterial and venous branches run in parallel within the same trabecula. However, the finer trabeculae have a more variegated distribution. Indeed, from the microscopic and mesoscopic point of view, trabecular arteries and veins do not have a similar arrangement (Table 4). In our study, in trabeculae we found more venous than arterial sections (in 161 out of 257 trabeculae studied there were more venous than arterial sections, and in 43 there were the same number).

However, these findings do not contradict the segmental distribution of the venous vessels at all. In this regard, it is important to remember that Dawson et al. (1986) found that "venous drainage did not overlap arterial segments, indicating that veins are intrasegmental".

In our material, the trabecular venous sections occupied an area 7.35 times greater than the trabecular arterial sections. Although we did not analyze the size of the macroscopic splenic vessels morphometrically, several studies seem to confirm that the diameter of the splenic vein is superior to that of the artery (Danno et al., 2009; Machálek et al., 1998; Silva et al., 2011; Silveira et al., 2009; Ünsal et al., 2006), which is in agreement with our observations of the microscopic vessels.

The 75 kDa low-affinity NGF receptor stains nerve endings, FDCs, the specialized cuboidal cells that cover the sheathed capillaries, some FRCs of the PALS and weakly other cells (Labouyrie et al., 1997; Steiniger et al., 2014a, b). Also anti-CD105 and anti-CD90 can react with the cuboidal cells that sheath capillaries. Now, these last ones do not allow to clearly identify these cells since they also react with other neighboring structures. Thus, taking into account all of the above, we can affirm that CD271 is a good marker for these cells. According to Steiniger et al. (2014a) about half of the red pulp capillaries are sheathed by cuboidal CD271+ cells. Although this statement has not been obtained by means of morphometry, it differs to some extent with our morphometric results (25.273% of the capillaries are CD271+).

In our material, the capillaries CD34+ and the SCs CD271+ were evenly distributed throughout the splenic cords. In all cases there were at least twice the number of vascular structures marked with anti-CD34 than with anti-CD271 and in 18 of the 21 cases there were at least three times the number of vascular structures marked with anti-CD34 than with anti-CD271, which effectively shows that most of the capillaries are not sheathed. However, there was no statistical pattern that establishes a ratio between the two, given the large numerical dispersion in each case.

Most of the macrophages associated to the cuboidal cells of the sheathed capillaries are CD68+ and CD163− (Steiniger et al., 2014a). On the other hand, many of the macrophages of the human red pulp are CD163+, CD91+, CD32+ and are related to erythrophagocytosis of senescent red blood cells and also to heme-hemopexin complexes and haemoglobin-haptoglobin complexes uptake (Ganz, 2012; Nagelkerke et al., 2018). Finally, the macrophages related to sheathed capillaries only from the perifollicular area of the human spleen express CD169 (Klaas and Crocker, 2012). Double staining for CD271 and CD169 in cryosections and in paraffin sections revealed that the sheath-associated macrophages were CD169++ only in perifollicular locations, but not in the remainder of the red pulp (Steiniger et al., 2014a).

In our material, the number of SCs CD169+ is three times less than the total number of SCs. Moreover, in all cases studied, there were more vascular structures marked with anti-CD271 than with anti-CD169. CD169+ SCs were found predominantly in the perifollicular area (Fig. 4B), exactly as it had already been described (Steiniger et al., 1997; Klaas and Crocker, 2012) and appeared more

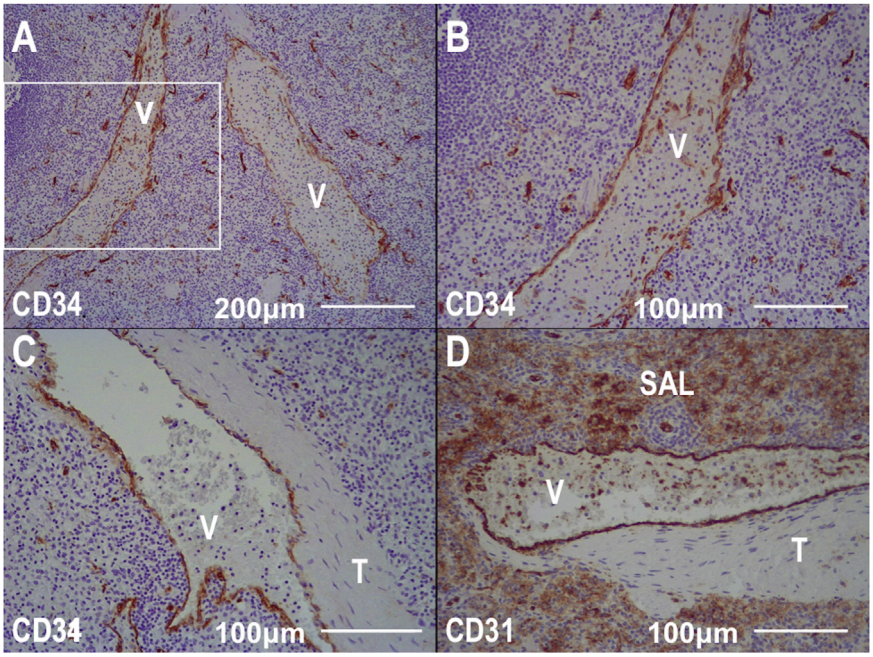


**Fig. 8.** (A) CD34. 10×. Two venules (V) stained with anti-CD34 delimited by a thin wall are observed. (B) CD34. 20×. Image boxed in A. The venule is devoid of muscular and connective parietal structures, in such a way that the endothelium is very close to the splenic cords. The venular endothelium is stained clearly with anti-CD34. In the surrounding red pulp thin capillaries stand out since the sinusoids are not marked with this immunostaining. (C) CD34. 20×. The upper right part of the vein (according to the orientation of the photomicrograph) is covered by a thick layer of dense connective tissue and, for all purposes, can be considered as part of a trabecular vein. However, the lower left part is completely devoid of muscular and connective parietal structures. This image agrees with our description that the splenic venules abruptly depart from the trabeculae (T) without there being a progressive thinning of their parietal structures. (D) CD31. 20×. Venous structure similar to that of C. Analogously the splenic venules abruptly depart from the trabecular. Observe how an accumulation of Sheath-Associated Lymphocytes (SAL) appears near the endothelium of the upper portion of the vein.

palely stained than the SCs CD271+. On the other hand, Korkusuz et al., 2002 says that the SCs are distributed diffusely throughout the red pulp, but we do not know if this refers to those that are nowadays stained with CD169.

In the histological studies of the human spleen there has long been controversy about the existence or absence of marginal sinus and even of the MZ as such. This problem is aggravated by the use of the spleen of rodents as a universally valid model. Van Krieken et al. (1985), using human spleens included in methylmethacrylate, did not find a structure comparable to the marginal sinus of rodents. On the other hand, this author considers that the PFZ (located between the white and red pulps) is not equivalent to the marginal sinus of the mice, probably being a peculiar territory of the red pulp. However, Schmidt et al. (1988) and Groom et al., (2002) affirm, with scanning electron microscopy, that the marginal sinus consists of a series of flattened, anastomosing vascular spaces between lymphatic nodule and marginal zone. Nevertheless there is the possibility that these flattened anastomosing vascular spaces may correspond to the perifollicular capillary plexus distended by the material used to make the cast.

Fujita et al. (1992) consider that open circulation also takes place in the marginal zone where the vessels of the "arteriolar capillary bundle" end. From this zone the blood would pass to the perimarginal sinusoids (many of them begin as open-ended tubes), providing a faster means of circulation. McCuskey and Reilly (1984) maintain a point of view similar, in a way, to the aforementioned.

More recently, the studies of Steiniger et al. on the human marginal and perimarginal zones and their relationship with different structures of the splenic microcirculation are significant. Steiniger et al. (2018a,b) describes a perifolicular capillary network (strongly positive for CD34) embedded in MRCs expressing MAdCAM-1, αSMA, and CD141. Similarly, Kusumi et al. (2015) describe an elaborate system of anastomosing capillaries in both the MZ and the superficial layer of the WP. In our study (Fig. 2A) these capillaries are outside the mantle and relatively distant from the perifollicular sinusoids which appear very palely stained with anti-CD34. It must be remembered that sinusoid endothelial cells are CD34+ only in the direct vicinity of splenic follicles (Steiniger et al., 2007). The spatial distribution and the size of the vessels marked with anti-CD34 was also identical to that observed in the work of Korkusuz et al. (2002).

Kraal et al. (1995) affirmed that the cells that react with anti-MAdCAm-1 are sinus-lining cells of the marginal zone of the mouse spleen. However, in our study, the cells that reacted with this antibody had a fibroblastoid-reticular morphology and did not seem to possess the proper features of endothelial cells (Fig. 4C).

Our results seem to indicate that there is no numerical relationship between the number of CD34+ capillaries and that of sinusoids. This agrees with the point of view according to which there is no anatomical continuity between the two structures (Steiniger et al., 2007). We could not find (with either anti-CD31 or anti-CD34) structures comparable to the "arterial labyrinth" which, according to Kashimura (1985) and Fujita et al. (1992), would allow a closed connection between arterial capillaries and sinusoids in restricted portions of the organ.

On the other hand, the slowing of the blood flow after entering the Billroth cords requires a sinusoidal vascular bed with greater capacity (since the flow that enters through the splenic artery is equal to that out of the splenic vein). In all our cases, the surface occupied by the CD8+ sinusoidal structures is much higher than that occupied by the CD34+ capillaries. Obviously, it is possible that those capillaries with diameters close to 6 µm, minimum diameter of capillary lumen according to Welsch and Deller (2013), have retracted below 5 µm as a consequence of the formalin fixation. In this way they would be undetectable in our measurements. With the same reasoning, there should also be a retraction of the sinusoidal surface, with which, quite possibly, the proportion between the surfaces of both types of vessels would be maintained. Moreover, in our 21 cases, the sinusoidal TA is, at least, 6.948 times greater than the capillary TA.

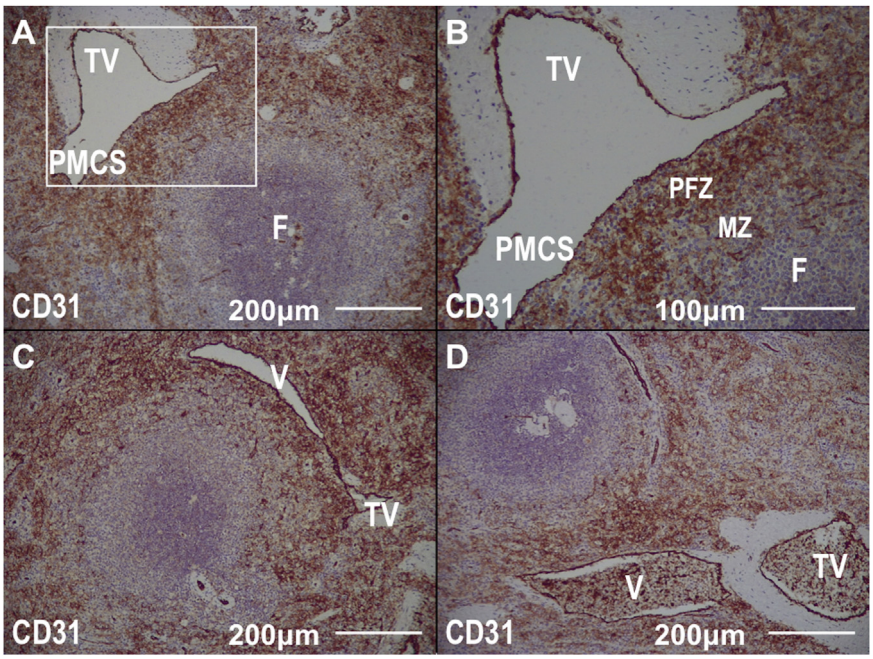


**Fig. 9.** (A) CD31. 10×. The follicle and its surrounding structures impose a curvilinear form on the splenic venule morphologically compatible with the so-called Peri-Marginal Cavernous Sinus (PMCS) in direct contact with the trabecular vein (TV). (B) CD31. 20×. At higher magnification, it is noted the dense microvascular pattern of the PFZ and also the fine capillary vessels that are part of the perifollicular capillary network. (C) CD31. 20×. Again, indicating how the venule compatible with PMCS is directly related to a trabecular vein. (D) CD31. 20×. Both the trabecular vein and the splenic venule contain numerous fusiform cells with a blurred outline that are clearly labeled with anti-CD31.
Abbreviations: F: Follicle. V: Splenic Venule.

Splenic venules have received scant attention both in regard to their structure and the antigenic profile of the endothelium. Contrary to the description by Steiniger and Barth (2000), in our material the venules were well developed (Fig. 8A). With light microscopy, they seemed to correspond to the vascular channels where the neighboring sinusoids converge (apparently they constitute a transition between both structures). No perivenular connective stroma was detected (Fig. 8B). They burst abruptly from the trabeculae without appreciating a progressive thinning of the trabecular stroma. The venular walls showed identical morphology both at the beginning and at the end of their route. Occasionally they run like tubular structures attached to the trabecula with one face covered by trabecular connective tissue and the other with an exclusively endothelial face (Fig. 8C, D). In other cases they appear as bulbous expansions or tubes with their major axis perpendicular to the trabecula.

The splenic venules presented a different immunohistochemical profile to the sinusoids, although, from a morphological point of view, the venules seemed to be a continuation of these. Unlike sinusoids, they presented a clear CD34 expression (Figs. 2B, 8 B, 8 C).

We observed wide venous spaces in numerous sections that sprouted abruptly from the trabecular veins and that were related to the perifollicular territory adopting a complementary curvilinear morphology in the contact zone of both structures (Fig. 9A, B, C, D).

These venous vessels had a histological structure, anatomical position and form similar to those of the perimarginal cavernous sinus described by Schmidt et al. (1988) and Groom et al. (2002). These authors observed with SEM that the endothelium that covers these structures presents a different morphology from the sinusoidal endothelium. In our material, with light microscopy, the only morphological difference that we detected was the greater height of the sinusoidal endothelium. However, the endothelium of these venules reacted with anti-CD34, while the sinusoidal endothelium did not present such immunoreaction with the only exception of a weak positivity in the perifollicular sinusoids (Steiniger et al., 2007). Since these structures are in anatomical continuity with the trabecular veins, we consider that they are simply venules whose morphology is determined by the presence of the follicle.

## 5. Conclusions

Numerical data provided by this work support that, possibly, the arterial and the venous vascular trees are two anatomically independent structures separated by splenic cords.

From a physiological point of view, we believe that more morphometric data would be necessary to construct a volumetric model of the splenic compartments in order to calculate the blood flow in each one of them.

On the other hand, the morphometric knowledge of splenic vascularization may have utility for diagnostic pathology. Although splenic vascular lesions are uncommon, their incidence has been increasing as a result of advances in diagnostic techniques (Uy et al., 2017). The technique and the morphometric data provided by this work may be useful to study quantitatively and to ease a correct differential diagnosis of complex and occasionally overlapping splenic vascular lesions such as hamartoma, peliosis, hemangioma, vascular malformations, lymphangioma-lymphangiomatosis, litoral cell angioma and sclerosing angiomatoid nodular transformation (Martel et al., 2004; Jindal et al., 2006; O'Malley, 2013; Sim et al., 2013; Ionannidis and Kahn, 2015; Peckova et al., 2016).

## Funding

The authors declare no conflict of interest. This work was supported by the Programa VLC-BIOCLINIC Subprograma A (Exp. 01-ESPUMA-JULIAN-RUIZ.2017-A) and Instituto de Salud Carlos III FEDER (Exp. PIE15/00013).

## Conflict of interest

None to declare.

## References


Buyssens, N., Paulus, G., Bourgeois, N., 1984. Ellipsoids in the human spleen. Virchows Arch. Pathol. Anat. 403, 27–40.

Christo, M.C., DiDio, L.J.A., 1997. Anatomical and surgical aspects of splenic segmentectomies. Ann. Anat. 179, 461–474.

Daniel, W.W., Cross, C.L., 2013. Biostatistics: A Foundation for Analysis in the Health Sciences, 10th edition. John Wiley & Sons, Inc., Hoboken, NJ, pp. 600–669.

Danno, K., Ikeda, M., Sekimoto, M., Sugimoto, T., Takemasa, I., Yamamoto, H., Doki, Y., Monden, M., Mori, M., 2009. Diameter of splenic vein is a risk factor for portal or splenic vein thrombosis after laparoscopic splenectomy. Surgery 145, 457–464.

Dawson, D.L., Molina, M.E., Scott-Conner, C.E., 1986. Venous segmentation of the human spleen. A corrosion cast study. Am. Surg. 52, 253–256.

Fujita, T., Kashimura, M., Adachi, K., 1992. Open and closed circulation in the spleen as evidenced by SEM of vascular casts. In: Motta, P.M., Murakami, T., Fujita, H. (Eds.), Scanning Electron Microscopy of Vascular Casts: Methods and Applications. Springer Science + Business Media, New York, pp. 111–122.

Ganz, T., 2012. Macrophages and systemic iron homeostasis. J. Innate Immunol. 4, 446–453.

García-Porrero, J.A., Lemes, A., 1988. Arterial segmentation and subsegmentation in the human spleen. Acta Anat. (Basel) 131, 276–283.

Ignjatovic, D., Stimec, B., Zivanovic, V., 2005. The basis for splenic segmental deartherialization: a post-mortem study. Surg. Radiol. Anat. 27, 15–18.

Ionannidis, I., Kahn, A.G., 2015. Splenic lymphangioma. Arch. Pathol. Lab. Med. 139, 279–282.

Irino, S., Murakami, T., Fujita, T., 1977. Open circulation in the human spleen. Dissection scanning electron microscopy of conductive-stained tissue and observation of resin vascular casts. Arch. Histol. 40, 297–304.

Jindal, R., Sullivan, R., Rodda, B., Arun, D., Hamady, M., Cheshire, N.J.W., 2006. Splenic malformation in a patient with Klippel-Trenaunay syndrome: a case report. J. Vasc. Surg. 43, 848–850.

Kashimura, M., 1985. Labyrinthine structure of arterial terminals in the human spleen, with special reference to "Closed circulation". A scanning electron microscope study. Arch. Histol. 48, 279–291.

Katritsis, E., Parashos, A., Papadopoulos, N., 1982. Arterial segmentation of the human spleen by post-mortem angiograms and corrosion-casts. Angiology 33, 720–727.

Klaas, M., Crocker, P.R., 2012. Sialoadhesin in recognition of self and non-self. Semin. Immunopathol. 34, 353–364.

Korkusuz, P., Dagdeviren, A., Aşan, E., 2002. Immunophenotypic analysis of human spleen compartments. Ann. Anat. 184, 431–441.

Kraal, G., Schornagel, K., Streeter, P.R., Holzmann, B., Butcher, E., 1995. Expression of the mucosal vascular addressin, MAdCAM-1, on sinus-lining cells in the spleen. Am. J. Pathol. 147, 763–771.

Kusumi, S., Koga, D., Kanda, T., Ushiki, T., 2015. Three-dimensional reconstruction of serial sections for analysis of the microvasculature of the white pulp and the marginal zone in the human spleen. Biomed. Res. 36, 195–203.

Labouyrie, E., Parrens, M., de Mascarel, A., Bloch, B., Merlio, J.P., 1997. Distribution of NGF receptors in normal and pathologic human lymphoid tissues. J. Neuroimmunol. 77, 161–173.

Machálek, L., Holibková, A., Tůma, J., Houserková, D., 1998. The size of the splenic hilus, diameter of the splenic artery and its branches in the human spleen. Acta Univ. Palacki. Olomuc. Fac. Med. 141, 45–48.

Martel, M., Cheuk, W., Lombardi, L., Lifschitz-Mercer, B., Chan, J.K.C., Rosai, J., 2004. Sclerosing angiomatoid nodular transformation (SANT): report of 25 cases of a distinctive benign splenic lesion. Am. J. Surg. Pathol. 28, 1268–1279.

McCuskey, R.S., Reilly, F.D., 1984. Hematopoietic system: spleen and bone marrow. A. Blood vessels and lymphatics of the spleen. In: Abramson, D.I., Dobrin, P.B. (Eds.), Blood Vessels and Lymphatics in Organ Systems. Academic Press, Orlando, pp. 698–704.

Mikhail, Y., Kamel, R., Nawar, N.N.Y., Rafla, M.F.M., 1979. Observations on the mode of termination and parenchymal distribution of the splenic artery with evidence of splenic lobation and segmentation. J. Anat. 128, 253–258.

Nagelkerke, S.Q., Bruggeman, Christine W., Ch.W., den Haan, J.M.M., Mul, E.P.J., van den Berg, T.K., van Bruggen, R., Kuijpers, T.W., 2018. Red pulp macrophages in the human spleen are a distinct cell population with a unique expression of Fc-γ receptors. Blood Adv. 2, 941–953.

O'Malley, D.P., 2013. Atlas of Spleen Pathology. Springer, New York.

O'Neill, A.S.G., Van den Berg, T.K., Mullen, G.D.E., 2012. Sialoadhesin — a macrophage-restricted marker of immunoregulation and inflammation. Immunology 138, 198–207.

Peckova, K., Michal, M., Hadravsky, L., Suster, S., Damjanov, I., Miesbauerova, M., Kazakov, D.V., Vernerova, Z., Michal, M., 2016. Littoral cell angioma of the spleen: a study of 25 cases with confirmation of frequent association with visceral malignancies. Histopathology 69, 762–774.

Pinkus, G.S., Warhol, M.J., O'Connor, E.M., Etheridge, C.L., Fujiwara, K., 1986. Immunohistochemical localization of smooth muscle myosin in human spleen, lymph node, and other lymphoid tissues. unique staining patterns in splenic white pulp and sinuses, lymphoid follicles, and certain vasculature, with ultrastructural correlations. Am. J. Pathol. 123, 440–453.

Satoh, T., Takeda, R., Oikawa, H., Satodate, R., 1997. Immunohistochemical and structural characteristics of the reticular framework of the white pulp and marginal zone in the human spleen. Anat. Rec. 249, 486–494.

Schmidt, E.E., MacDonald, I.C., Groom, A.C., 1988. Microcirculatory pathways in normal human spleen, demonstrated by scanning electron microscopy of corrosion casts. Am. J. Anat. 181, 253–266.

Schmidt, E.E., MacDonald, I.C., Groom, A.C., 1991. Changes in splenic microcirculatory pathways in chronic idiopathic thrombocytopenic purpura. Blood 78, 1485–1489.

Silva, L.F., Silveira, L.M., Timbó, P.S., Pinheiro, S.R., Barros, L.V., da Silva Filho, A.R., 2011. Morfometric study of arterial branching of the spleen compared to radiological study. Rev. Col. Bras. Cir. 38, 181–185.

Silveira, L.A., Silveira, F.B.C., Fazan, V.P.S., 2009. Arterial diameter of the celiac trunk and its branches. Anatomical study. Acta Cir. Bras. 24, 43–47.

Sim, J., Ahn, H.I., Han, H., Jun, Y.J., Rehman, A., Jang, S.M., Jang, K.S., Paik, S.S., 2013. Splenic hamartoma: a case report and review of the literature. World J. Clin. Cases 1, 217–219.

Steiniger, B.S., 2015. Human spleen microanatomy: why mice do not suffice. Immunology 145, 334–346.

Steiniger, B., Barth, P., 2000. Microanatomy and function of the spleen. Adv. Anat. Embryol. Cell Biol. 151, 1–100.

Steiniger, B., Barth, P., Herbst, T.B., Hartnell, A., Crocker, P.R., 1997. The species-specific structure of microanatomical compartments in the human spleen: strongly sialoadhesin-positive macrophages occur in the perifollicular zone, but not in the marginal zone. Immunology 92, 307–316.

Steiniger, B., Barth, P., Hellinger, A., 2001. The perifollicular and marginal zones of the human splenic white pulp: do fibroblasts guide lymphocyte immigration? Am. J. Pathol. 159, 501–512.

Steiniger, B., Timphus, E.M., Barth, P.J., 2006. The splenic marginal zone in humans and rodents: an enigmatic compartment and its inhabitants. Histochem. Cell Biol. 126, 641–648.

Steiniger, B., Stachniss, V., Schwarzbach, H., Barth, P.J., 2007. Phenotypic differences between red pulp capillary and sinusoidal endothelia help localizing the open splenic circulation in humans. Histochem. Cell Biol. 128, 391–398.

Steiniger, B., Bette, M., Schwarzbach, H., 2011. The open microcirculation in human spleens: a three-dimensional approach. J. Histochem. Cytochem. 59, 639–648.

Steiniger, B., Seiler, A., Lampp, K., Wilhelmi, V., Stachniss, V., 2014a. B lymphocyte compartments in the human splenic red pulp: capillary sheaths and periarteriolar regions. Histochem. Cell Biol. 141, 507–518.

Steiniger, B.S., Wilhelmi, V., Seiler, A., Lampp, K., Stachniss, V., 2014b. Heterogeneity of stromal cells in the human splenic white pulp. Fibroblastic reticulum cells, follicular dendritic cells and a third superficial stromal cell type. Immunology 143, 462–477.

Steiniger, B.S., Ulrich, Ch, Berthold, M., Guthe, M., Lobachev, O., 2018a. Capillary networks and follicular marginal zones in human spleens. Three-dimensional models based on immunostained serial sections. PLoS One 13 (2), e0191019.

Steiniger, B.S., Wilhelmi, V., Berthold, M., Guthe, M., Lobachev, O., 2018b. Locating human splenic capillary sheaths in virtual reality. Sci. Rep. 8, 15720, http://dx.doi.org/10.1038/s41598-018-34105-3.

Stuart, A.E., Warford, A., 1983. Staining of human splenic sinusoids and demonstration of unusual banded structures by monoclonal antisera. J. Clin. Pathol. 36, 1176–1180.

Tablin, F., Chamberlain, J.K., Weiss, L., 2002. The microanatomy of the mammalian spleen. Mechanisms of splenic clearance. In: Bowdler, A.J. (Ed.), The Complete Spleen. Structure, Function, and Clinical Disorders. , 2nd edition. Springer Science + Business Media, New York, pp. 11–21.

Ünsal, N.H., Erden, A., Erden, I., 2006. Evaluation of the splenic vein diameter and longitudinal size of the spleen in patients with Gamna-Gandy bodies. Diagn. Interv. Radiol. 12, 125–128.

Uy, P.P.D., Francisco, D.M., Trivedi, A., O'Loughlin, M., Wu, G.Y., 2017. Vascular diseases of the spleen: a review. J. Clin. Transl. Hepatol. 5, 152–164.

Van den Berg, T.K., Brevé, J.J.P., Damoiseaux, J.G.M.C., Döpp, E.A., Kelm, S., Crocker, P.R., Dijkstra, Ch.D., Kraal, G., 1992. Sialoadhesin on macrophages: its identification as a lymphocyte adhesion molecule. J. Exp. Med. 176, 647–655.

Van Krieken, J.H.J.M., te Velde, J., 1986. Immunohistology of the human spleen: an inventory of the localization of lymphocyte subpopulations. Histopathology 10, 285–294.

Van Krieken, J.H.J.M., te Velde, J., 1988. Normal histology of the human spleen. Am. J. Surg. Pathol. 12, 777–785.

Van Krieken, J.H., te Velde, J., Kleiverda, K., Leenheers-Binnendijk, L., Van de Velde, C.J., 1985. The human spleen: a histological study in splenectomy specimens embedded in methylmethacrylate. Histopathology 9, 571–585.

Weill, J.C., Weller, S., Reynaud, C.A., 2009. Human marginal zone B cells. Annu. Rev. Immunol. 27, 267–285.

Welsch, U., Deller, Th., 2013. Sobotta Histologia. Editorial Médica Panamericana, México.